

PEP INSERTION QUADRUPOLE DESIGN FEATURES*

Robert T. Avery, Thomas Chan, Klaus Halbach,
Robert Main, and Jack Tanabe**

Abstract

The insertion quadrupoles for the PEP storage ring must have a very uniform gradient to focus the circulating beams to a very small size at the interaction point for high luminosity. Quads have been built which achieve the desired field within the full pole aperture radius to approximately one part in 10^4 . The design features which permitted this achievement are described.

Precise Field Quality Required

The quality required varies for different beam energies and lattice settings. Typical criteria for the integrated relative field error for all rays within the maximum (10 σ) beam envelope of Figure 1 was

$$\int \frac{\Delta B}{B} dx \leq 1 \times 10^{-4} \quad \text{over total length including end fringe fields.}$$

$$\text{and } \int \frac{\Delta B}{B} dx \leq 5 \times 10^{-4} \quad \text{over any 20\% of effective length.}$$

Originally less vertical coupling of betatron oscillations was assumed, requiring precise field out to only 67 mm radius. Later, experience from SPEAR suggested that 100% vertical coupling should be assumed under certain conditions, thus requiring precise field out to 83 mm radius (slightly greater than the magnet aperture radius of 80 mm). At that stage, it was difficult to increase the aperture of the magnet so we, in essence, were forced to achieve the precise field quality over a larger region than originally anticipated.

The stringent field quality requirement can be appreciated by realizing that the Q1/Q2 pair must focus all beam rays within a very small spot (e.g., $\sigma_y^* = \pm .055 \text{ mm} = \pm .002 \text{ inch}$) at a distance away of 10-15 meters, as pictured in Figure 2.

Design Features

The major design features, some novel, that were incorporated (Figure 3) to achieve the desired performance are:

1. Optimized Pole Contour. The pole contour was computer-optimized using the MIRT magnetostatic program¹ together with a quad/dipole conformal transformation² (Fig. 4) for greater precision. A maximum computed relative field error of $< 2 \times 10^{-4}$ was achieved over the precise field envelope.
2. Two-pole Lamination. A single parting plane (each lamination includes two poles) minimize pole positioning errors.
3. High-Quality Steel. The magnets were fabricated of 1.5 mm (.060") mild steel sheet that subsequently was decarburized and fully annealed to minimize hysteresis effects.
4. Precise Punching. The punch and die were wire electric-discharge machined from hardened tool steel.

Lamination pole contour errors were typically $< .012 \text{ mm} (.0005")$ and gap between adjacent poles typically varied $< .025 \text{ mm} (.001")$.

5. Accurate Stacking. Lamination stacking was done on a granite surface plate using a pair of granite straight-edges for transverse alignment (Fig. 5). The laminations were compressed by hydraulic jacks "pulling" on the bars of the magnet; then the bars were bolted and doweled to the 50 mm (2.0") thick end plates of the magnet, all with the magnet core still aligned by the granite pieces. Incidentally, granite pieces are relatively inexpensive for a stacking fixture and can be used later for general shop use.

6. No Welding. Welding distortion was avoided. Instead, the laminations were retained relative to the structural bars by injecting steel-loaded epoxy into V-grooves (Fig. 6) while the core was still aligned by the granite. Completed cores were straight $\sim .05 \text{ mm} (.002")$.

7. Rigid Support Girder. The core would sag almost 0.5 mm (.020") if simply supported at the ends. Instead, the lower core was supported by eight jacks surmounting a rigid steel girder which became part of the final magnet assembly (Fig. 7). The median plane was adjusted to be flat within $.025 \text{ mm} (.001")$.

8. Accurate Core Alignment. The upper core was aligned to the lower core by means of dowels in V-grooves at the median plane (Fig. 3). Shims could be inserted on one or both sides of each vee and different shims could be used on left and right grooves, providing vertical, horizontal and rotational (or any combination) motion of the upper core relative to the lower. Measurements of sextupole and octupole field errors indicated which type of motion was needed.³

9. Tailored Pole Ends. Pole tip ends were removable and had a 35° chamfer to approximately correct for end effect in the magnet. After initial magnet measurement, the contour of each tip (4 poles x 2 ends = 8 pieces) could be individually tailored to a 15-point contour that not only overcame residual end effects at both ends of the magnet but also compensated for any small residual error through the middle portion of the magnet.

10. Mirror Plates. Mirror plates and steel coil covers were used to minimize effects due to possible nearby magnetic objects. The split plane of the mirror plates was located at 45° (where flux density is zero).

11. Two Coils per Pole. The throat between adjacent poles on a lamination limit the size of coils that can be assembled onto each pole. Reasonable current densities (and power consumption) were achieved for these magnets by using two coils per pole--one having two layers of four turns each and the second having one layer of five turns.

12. Main/Auxiliary Coils. All 24 insertion quadrupoles are connected electrically in series with the PEP ring bend magnets; otherwise, more stringent power supply regulation would be required. Auxiliary coils are provided for trimming the strength of individual magnets. All conductors are hollow-core aluminum. Main conductor size was too large to use "saddle" coil returns so "racetrack" returns were used instead.

*This work was supported by the Office of High Energy and Nuclear Physics Division of the U.S. Department of Energy under contract No. W-7405-ENG-48.

**Lawrence Berkeley Laboratory, Berkeley, CA 94720

Measured Results

An improved system⁴⁾ was used to measure the magnetic field quality of these magnets. The results for a typical magnet are shown in Figures 8 and 9. These indicate that the desired field quality has been substantially achieved.

The gradient x length product was measured⁵⁾. Then, each magnet was split on the median plane for installation of the UHV chamber⁶⁾. Measurements of $n = 3$ & 4 field error coefficients indicated no significant change in magnetic field quality due to splitting.

Principal Parameters

	Q1	Q2
Quantity	12	12
Core length, meters	1.95	1.45
Magnetic length, meters	2.03	1.53
Poletip field @ 18 GeV, Tesla	0.52	0.53
Rated Main current	1319	1319
Current Density (@ 1319 A), A/mm ²	2.09	2.09
Voltage (@ 1319 A), volts	16.2	12.9
Power (@ 1319A), kW	21.4	17.0
Rated auxiliary current, A	±65	±65
Overall weight, metric tons	8.8	6.8

Acknowledgments

We acknowledge the help of so many colleagues at LBL and SLAC that it is impossible to mention them individually. The skilled craftsmanship of the LBL Mechanical Shops has been particularly appreciated.

References

1. K. Halbach, "Program of Inversion of System Analysis and Its Application to the Design of Magnets," Proc. 2nd Intl. Conf. Magnet Technology, Oxford. (1967).
2. K. Halbach, "Application of Conformal Mapping to Evaluation and Design of Magnets Containing Iron with Non-Linear B(H) Characteristics", Nucl. Inst. & Meth., Vol. 64, p. 275, (1968).
3. K. Halbach, "First Order Perturbation Effects in Iron-Dominated Two-Dimensional Symmetrical Multipoles"; Nucl. Instr. & Methods, Vol. 74, p. 147 (1969). Also K. Halbach and R. Yourd, "Tables and Graphs of First Order Perturbation Effects of Iron Dominated Two-Dimensional Multipoles"; USRL-18916 (1969).
4. R.M. Main, J. Tanabe and K. Halbach, "Measurements and Corrections of the PEP Interaction Region Quadrupole Magnets"; Paper J-5 at this conference.
5. D. Reagan, "A Device to Measure Gradient-Length Product"; Paper J-15 at this conference. Measurements performed by J. Dorst.
6. Courtesy of J. Cobb, G. Fischer, and T. Winch, SLAC.

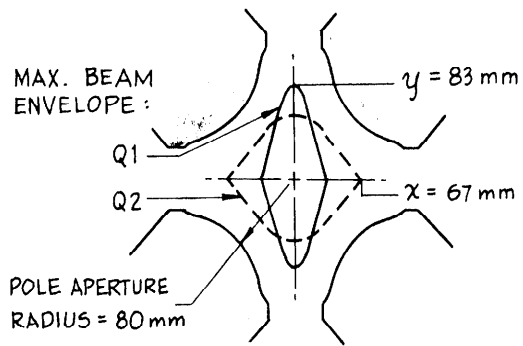


Fig. 1. Quad bore showing 10σ maximum beam envelope requiring precise field.

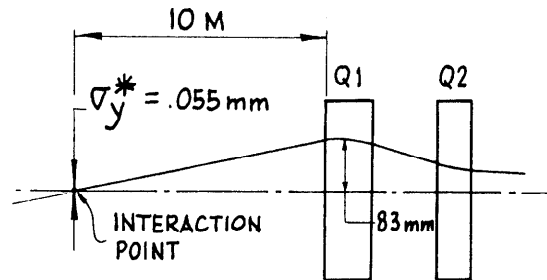


Fig. 2. Vertical beam envelope through Q1/Q2 insertion quads.

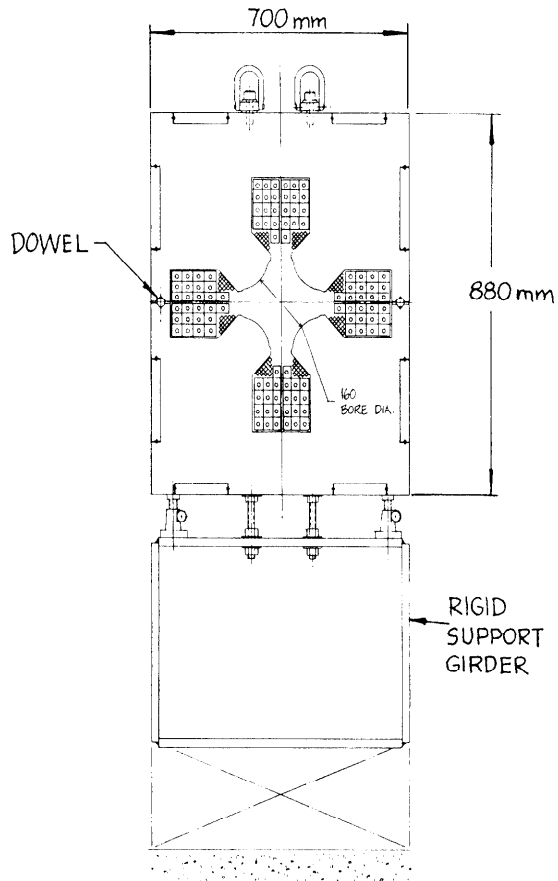


Fig. 3. Typical cross-section.

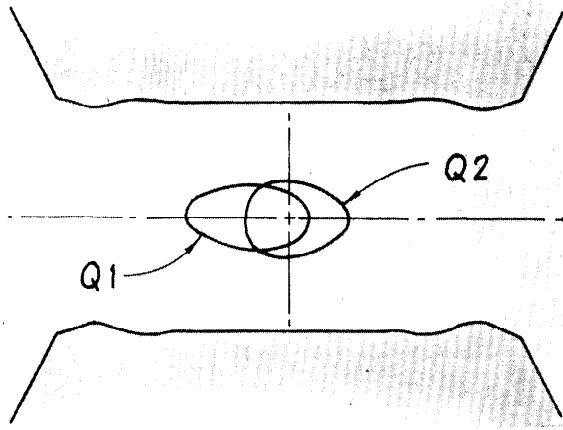


Fig. 4. Dipole conformal transformation of quadrupole bore showing transformed precise field regions.

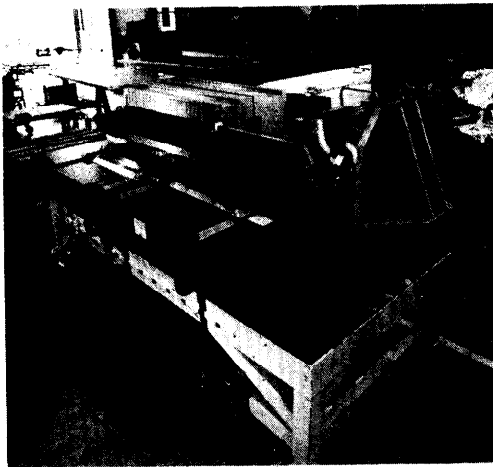


Fig. 5. Lamination stacking using granite surface plate and straight-edges.

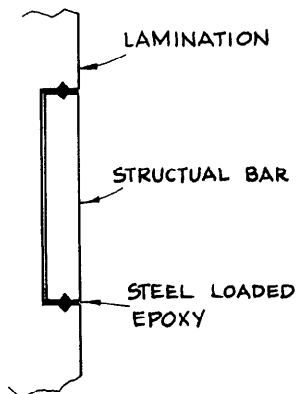


Fig. 6. Retention of Laminations by steel-loaded epoxy.

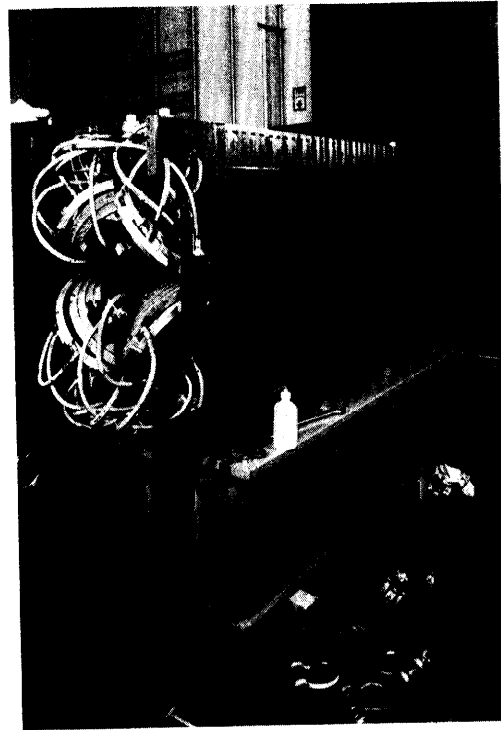


Fig. 7. Complete magnet (mirror plate and covers removed) aligned on support girder.

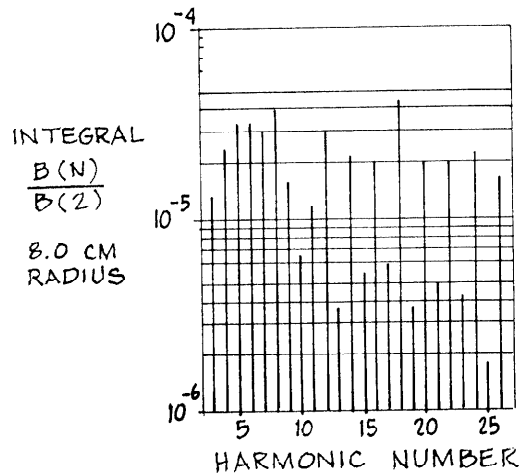


Fig. 8. Harmonic multipole coefficients normalized at full aperture radius (80 mm) to quadrupole magnitude for typical magnet.

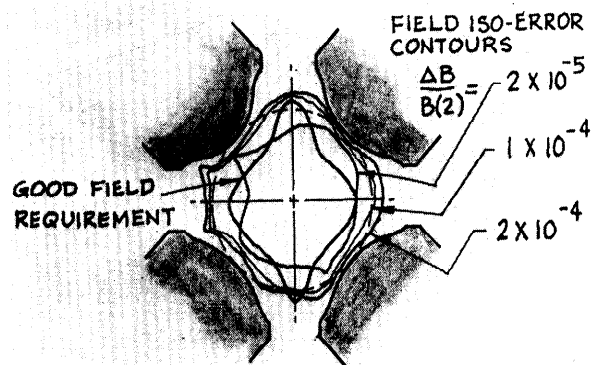


Fig. 9. Field error contours (based on data of Fig. 8).